



LAWRENCE  
LIVERMORE  
NATIONAL  
LABORATORY

# First Principles Study of Nanodiamond Optical and Electronic Properties

Jean-Yves Raty, Giulia Galli

November 29, 2004

Computer Physics Communications

## **Disclaimer**

---

This document was prepared as an account of work sponsored by an agency of the United States Government. Neither the United States Government nor the University of California nor any of their employees, makes any warranty, express or implied, or assumes any legal liability or responsibility for the accuracy, completeness, or usefulness of any information, apparatus, product, or process disclosed, or represents that its use would not infringe privately owned rights. Reference herein to any specific commercial product, process, or service by trade name, trademark, manufacturer, or otherwise, does not necessarily constitute or imply its endorsement, recommendation, or favoring by the United States Government or the University of California. The views and opinions of authors expressed herein do not necessarily state or reflect those of the United States Government or the University of California, and shall not be used for advertising or product endorsement purposes.

# First principle study of nanodiamonds optical and electronic properties

Jean-Yves Raty <sup>a,✉</sup> and Giulia Galli <sup>b</sup>

<sup>a</sup>*Département de Physique, Université de Liège, 4000 Sart-Tilman, Belgium*

<sup>b</sup>*Lawrence Livermore National Laboratory, P.O. Box 808, Livermore CA94550*

---

## Abstract

Nanometer sized diamond has been found in meteorites, proto-planetary nebulae and interstellar dusts, as well as in residues of detonation and in diamond films. Remarkably, the size distribution of diamond nanoparticles appears to be peaked around 2-5 nm, and to be largely independent of preparation conditions. Using ab-initio calculations, we have shown that in this size range nanodiamond has a fullerene-like surface and, unlike silicon and germanium, exhibits very weak quantum confinement effects. We called these carbon nanoparticles bucky-diamonds: their atomic structure, predicted by simulations, is consistent with many experimental findings. In addition, we carried out calculations of the stability of nanodiamond which provided a unifying explanation of its size distribution in extra-terrestrial samples, and in ultra-crystalline diamond films.

*Key words:* nanodiamond, ab initio, optical properties, fullerene

*PACS:* code1, code2

---

---

<sup>✉</sup> Corresponding Author:

*Email address:* jyraty@ulg.ac.be (Jean-Yves Raty).

## 1 Introduction

Nanometer sized diamond is a constituent of diverse systems ranging from interstellar dusts and meteorites [1] to carbonaceous residues of detonations [2] and diamond-like films[3]. Many of the properties of bulk diamond have been well understood for decades, those of nanodiamond are mostly unexplored.

The characterization of nanodiamonds from both the sky and the earth has revealed interesting, common features, in particular the presence of graphitic-like sites, possibly at the surface [4]. For example, UNCD films are believed to contain 2-5% of sp<sup>2</sup> bonded carbons, supposedly at grain boundaries and less than 1 % hydrogen. Aleksenskii et al. [4] performed a structural study of UDD using X-ray diffraction and small angle X-ray scattering and found that the majority of nanodiamond has a core size of about 4 nm, with a surface covered by a mixture of sp<sup>2</sup> and sp<sup>3</sup> bonded carbon atoms.

In this paper, we present a theoretical study showing that diamond has unique properties not only as a bulk material but also at the nanoscale, where size reduction and surface reconstruction effects are fundamentally different from those found , e.g. in Si and Ge [5]. Using ab-initio calculations within the Density Functional Theory (DFT) framework, we showed that nanoscale diamond obtained by detonation as well as found in meteorites indeed has a diamond core with a fullerene-like surface reconstruction and we have called these carbon particles bucky diamonds [6]. We give a description of bucky diamonds in Section 4, after describing the properties of hydrogenated nanodiamonds smaller than ~2 nm in Section 3. Finally, we have study the relative stability of nanodiamonds as a function of size and of the surface hydrogen coverage in section 5. Our results show that as the size of dia-

mond is reduced to about 3 nm, it is energetically more favorable for this material to have bare, reconstructed surfaces than hydrogenated surfaces. This inability to retain hydrogen at the surface may then prevent the growth of larger grains [7].

## 2 Theory

In our DFT calculations, performed both within the generalized gradient approximation (GGA) and the time dependent local density approximation (TDLDA), we used a pseudopotential, plane wave approach. We chose the planewaves energy cutoff equal to 35 Rydberg and imposed the spacing between periodic replica of a single cluster to be at least equal to 8 Å. We checked that under these conditions, the interatomic distances and HOMO-LUMO energy separation are converged to less than 0.1 Å and 0.1 eV, respectively. All structures were fully relaxed, using Car-Parrinello molecular dynamics [8] at low temperature, until the residual forces got less than 1 Ry/bohr. These conditions allowed us to accurately compute the ground state geometry and electronic structure of clusters containing up to 447 atoms (C<sub>275</sub>H<sub>172</sub>). Those calculations were performed using the GP code<sup>1</sup>.

Due to well known shortcomings of local density approximations to describe the excited states of systems, and so for, the energy gap, we use a the time dependent local density approximation to improve the description of the excited states. We follow the linear response formulation of Casida [9] in the ABINIT code implementation [10].

---

<sup>1</sup> G.P Code, F. Gygi, LLNL (1999-2001).

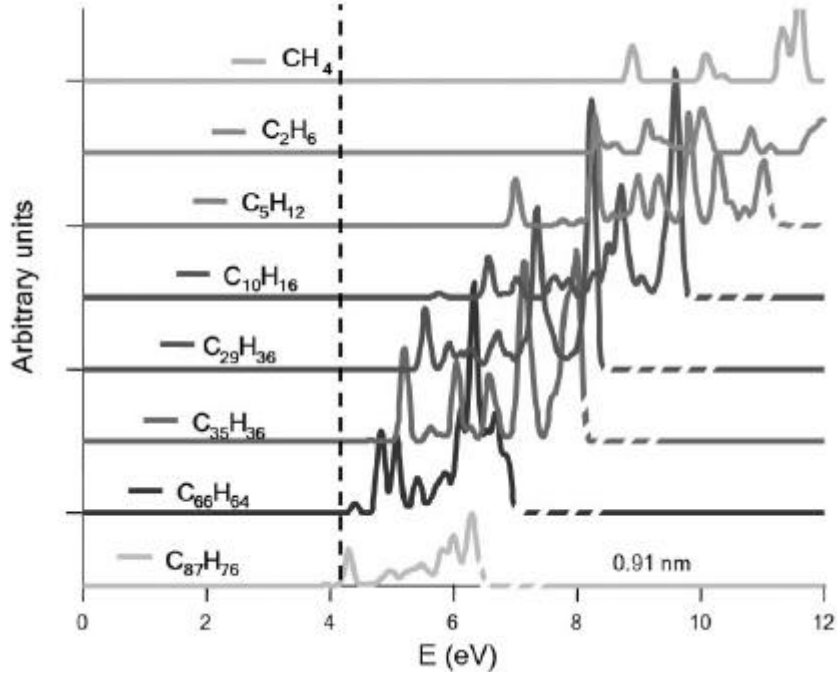


Fig. 1. Absorption spectra of fully hydrogenated nanodiamonds up to 1 nm in diameter. At least 600 excitations have been included in the linear response treatment to ensure the convergence of the spectra on a range of minimum 2 eV above the onset of the absorption. The spectra are truncated at high energy (dashes). The vertical dashed line corresponds to the absorption gap of bulk diamond with the same level of accuracy and converged with respect to k-points.

### 3 Hydrogenated nanodiamonds absorption spectra

The nanodiamonds structures are generated from a spherically truncated diamond slab where all the dangling bonds are saturated with hydrogen atoms. Upon relaxation, strong angular distortions at the surface occur and we note that, to the contrary of the other group IV nanoclusters, size reduction to a few nanometers induces a tensile stress to act on the structure. This results in a significant increase, up to 6% in comparison to bulk, of the C-C bond length.

The computed absorption spectra are shown on Fig.1. We note a very rapid de-

crease of the absorption gap value which gets similar to the computed bulk value for particles about 1 nanometer in diameter. This indicates the absence of quantum confinement effect for particles larger than 1-2 nanometers as was established in ref. [6]. The oscillator strength of the first allowed transition is also rapidly decreasing, in agreement with the formation of an indirect gap in the bulk limit case. Interestingly, the onset of absorption can even appear at energies that are smaller than the bulk absorption gap for clusters diameters of the order of 1 nm.

#### **4 Surface reconstructions**

Depending on preparation conditions, and especially on heating treatments of the samples, nanodiamonds produced experimentally may not have an ideal diamond surface saturated by hydrogen atoms, but rather exhibit reconstructed surfaces. To investigate the effect of surface reconstruction on hydrogenated nanoparticles, we studied some representative cases. Starting from the unrelaxed, fully hydrogenated, geometries, we removed pairs of hydrogens whose interatomic distances were within 5 % of the  $H_2$  bond length (see Fig.2). All surfaces spontaneously reconstructed at low temperature but the reconstruction induced almost no change in the GGA Homo-Lumo gap values.

The effect of surface reconstruction is more important on the TDLDA absorption spectra, as the example is given on Fig.3. The absorption gap value, as defined by the first non-zero oscillator strength transition is typically reduced by about 0.5 eV upon reconstruction. The overall shape of the absorption spectra is however quite unaffected by the reconstruction of the surface.

This effect of reducing the gap can be qualitatively guessed from the HOMO and

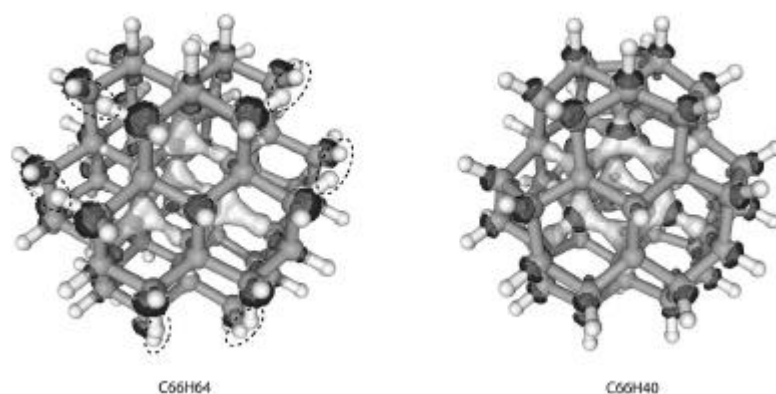


Fig. 2. Fully hydrogenated 66 carbon atom cluster (left) and (100) reconstructed cluster (right). The (100) reconstruction occurs spontaneously upon removal of pairs of hydrogen atoms, such as those circle on the left. The HOMO and LUMO are represented by the light- and dark isosurfaces respectively and are drawn at 33% of their maximal value.

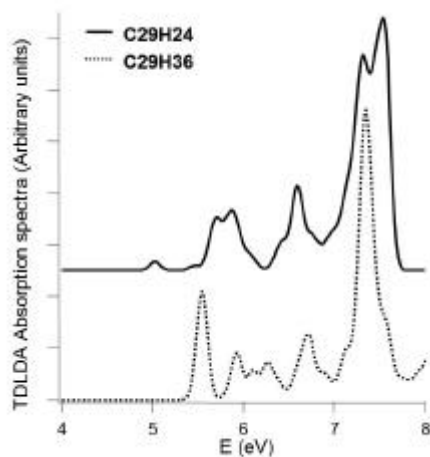


Fig. 3. Absorption spectra of unreconstructed and (100) reconstructed C29 clusters.

LUMO geometries, as on the example from Fig. 2. Upon reconstruction, the HOMO gets somewhat extended towards the surface but the LUMO is significantly transferred from surface atoms to deeper core atoms.



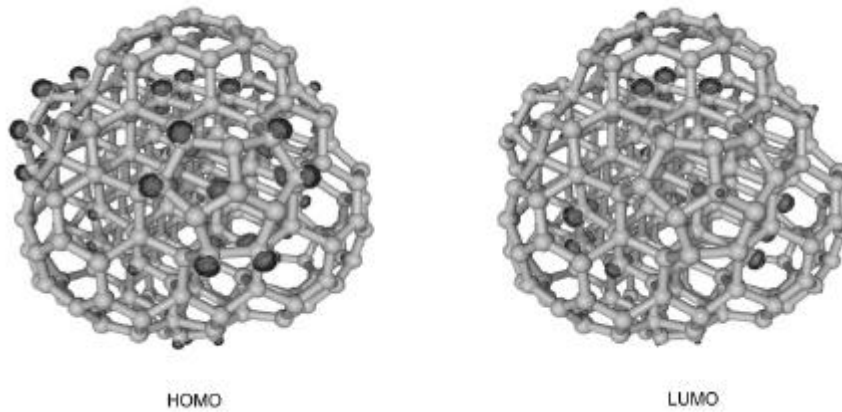


Fig. 4. C275 "Buckydiamond" HOMO and LUMO (Kohn-sham) states. The isosurfaces are drawn at 25% of their maximal value.

## 5 Bucky-diamonds

For a series of particles with diameters up to 1.5 nm, we explicitly studied the geometry of surface reconstruction, in the absence of passivants. For all clusters we observe the graphitization of the (111) facets as well as the well known (100) reconstruction forming dimers on the surface. These combined effects create caps whose structure, and curvature is similar to some fullerenes. These have been previously called "bucky diamonds"[6]. We evidenced similar reconstructions for larger clusters (up to 3 nanometers) using tight binding monte carlo simulation [11]. For all clusters studied ab initio, the HOMO and LUMO states are located at the interface between the diamond core and the reconstructed (111) facets. On Fig.4 one can see that the HOMO has most of its contribution below the fullerene-like caps and at the edges of surface pentagons, while the LUMO is almost entirely located below the fullerenic caps and on the surface hexagons.

These surface states and reconstructions are indeed compatible with previously recorded X-ray absorption spectra [6].

It is interesting to note that the barrier between the ideal - bare- surface structure and the reconstructed surface is size dependent and increases as the size of the nanoparticle is increased, to become of the order of several tens of eV, as found in bulk diamond[12].

## 6 Chemical potential stability study

Having established the atomic and electronic structure of both hydrogenated and bare nanodiamonds, we studied the relative stability of nanoparticles with the same carbon content but different hydrogen coverage, as a function of size, using a grand canonical formalism. The formation energy of a carbon particle is defined as:

$$E_{formation} = E_{total} - \mu_C N_C - \mu_H N_H - E_{vib}$$

Here  $N_x$  are the numbers of C or H atoms and  $\mu_x$  is their respective chemical potential;  $E_{vib}$  and  $E_{total}$  are the vibrational and the total energy of a nanoparticle, respectively, obtained within DFT. The formation energy thus expresses the difference in energy between a nanoparticle and a reservoir of carbon and hydrogen atoms whose energy is  $\mu_x$ . In our calculations, we considered five core sizes containing 29, 66, 147, 211 and 275 C atoms and for all of them we found that the stability sequence of the particles with different surface structures is the same as a function of  $\mu_H$ . In all five cases, in going from the  $\text{CH}_4$  chemical potential to lower values, the stable structures are, in order of increasing stability, nanoparticles with fully hydrogenated surfaces, those with (111) reconstructed, hydrogenated surfaces and those with bare, reconstructed surfaces. Our results for the formation energy of two specific diamond clusters (with 66 and 275 C atoms, respectively) as a function of the hydrogen chemical potential are shown in Fig.5. This figure indicates that the

difference in formation energy between particles with hydrogenated surfaces and those with bare surfaces is rapidly decreasing as the size of the nanoparticle is increased. This suggests that there exist a size in the nanometer range where a reversal of stability between hydrogenated and bare nanoparticles will occur and bucky diamonds (or parent structures) will become more stable than diamond nanoparticles with hydrogenated, reconstructed surfaces.

The computed difference in formation energy ( $\Delta$ ) between the stable hydrogenated structure and the bare diamond nanoparticle as a function of size is shown in Fig.6, where we assumed that  $\Delta$  is dependent only on the number of surface carbon atoms. With this assumption,

$$\Delta = E_{formation,bare}^{3/2} - E_{formation,stable}^{3/2}$$

is almost linear with the particle diameter. Our results show that for all values of the H chemical potential,  $\Delta$  becomes negative when the diameter of the nanoparticle is comprised between 2 and 3 nanometers. In other words,  $\Delta$  does not depend in any significant way on the hydrogen chemical potential, and thus to a large extent on different experimental synthesis conditions.

Our calculations show that between 2 and 3 nm, it is energetically more favorable for nanodiamond to have a bucky diamond-like structure and bare unreconstructed surfaces than having hydrogen at the surface. The presence of hydrogen is a necessary condition for the growth of diamond; therefore the release of surface hydrogen from growing nanodiamonds should result in the premature end of the growth of bulk samples between 2 and 3 nm. These findings help explain why nanodiamond size distributions are peaked around the same size, about 3 nm, irrespective of the preparation method used to generate the nanoparticles. Although our calculations

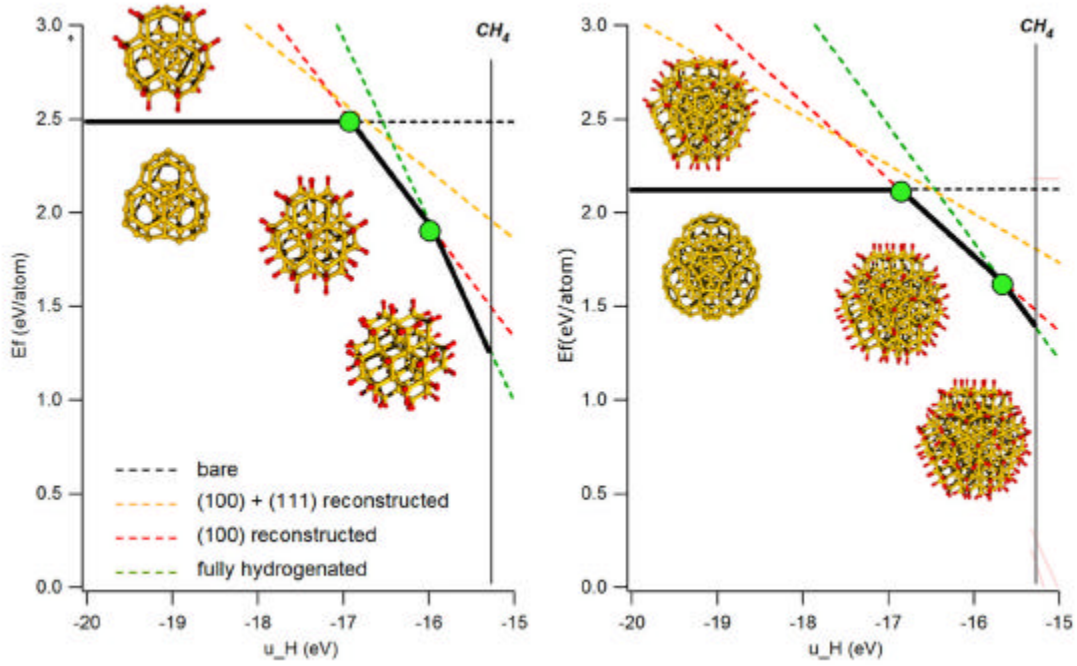


Fig. 5. Formation energy of nanodiamonds with different hydrogen coverage and different core sizes (66 C atom and 275 Carbon atoms on the left and right hand sides, respectively), as a function of the hydrogen chemical potential, which mimic different preparation conditions.

cannot establish the exact size at which the crossover between hydrogenated and bare, reconstructed surfaces occur, they provide a robust, qualitative explanation of why the crossover occurs in the few nanometers range, and why it is the same irrespective of preparation conditions.

Based on the simple thermodynamic mechanism presented here, one might argue that it would be impossible to grow diamond on a micro- or macroscopic scale. To address this issue, it is necessary to compare the formation energies of nanodiamonds of various sizes with those of flat diamond surfaces. This comparison indicates that at the highest values of the H chemical potential (-15.5 eV) considered in our study, the infinite (100) surface is more stable than any nanodiamond,

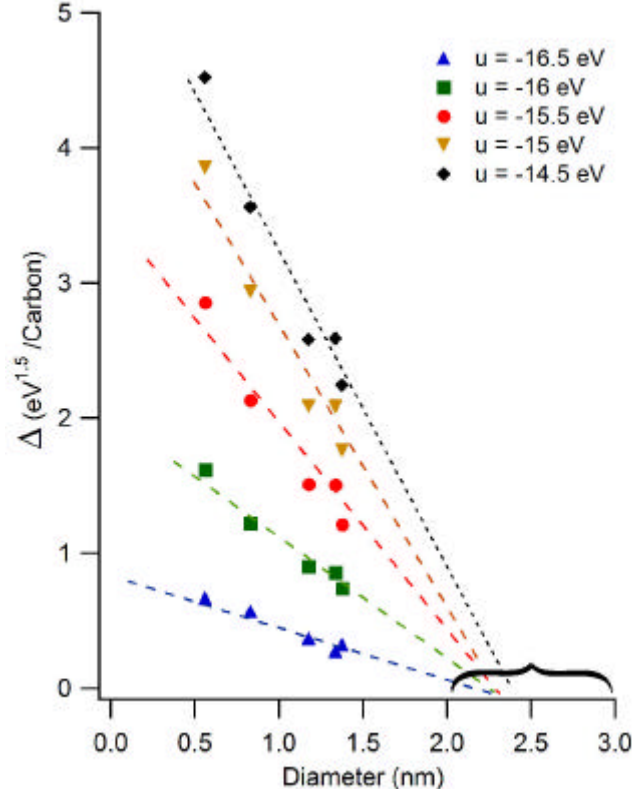


Fig. 6. Difference in formation energy between nanodiamonds with fully reconstructed surfaces and the most stable structure found for a given value of the hydrogen chemical potential ( $u$ ), as a function of the nanoparticle size.

while at lower chemical potential, there exist a critical diameter above which the nanodiamond clusters are the most stable structure. For instance at a chemical potential value of -16.5 eV, if the particle grows to a diameter larger than 2.5 nm, then it becomes more stable than a bulk surface. These numerical results help explain how, by varying the hydrogen pressure (and thus the hydrogen chemical potential) in a CVD reactor, one can deposit either microcrystalline or ultrananocrystalline diamond films.

## 7 Conclusions

In summary, using ab-initio methods with no adjustable parameters, we have proposed an explanation for the ultradispersity of diamond at the nanoscale which relies on simple thermodynamic arguments. We have shown that depending on the temperature and pressure of the hydrogen and carbon gases used in diamond growth processes, diamond will grow into nanoparticles with reconstructed, non hydrogenated surfaces of about 3 nm or into microcrystallites, if the typical conditions of diamond CVD growth are met. Our results, together with the proposed geometry of bucky diamond will help build structural models of UNCD and UDD films which can be used to study mechanical properties of these systems, as well as their interfaces with biological molecules.

## 8 Acknowledgments

This work was performed under the auspices of the U.S. Department of Energy at the University of California/Lawrence Livermore National Laboratory under Contract No. W-7405-Eng-48. JYR acknowledges support from the FNRS and the NOMADE-Region wallonne contract.

## References

- [1] R. Lewis, M. Tang, J. Wacker, E. Anders, E. Steel, Interstellar diamonds in meteorites, *Nature* 326 (1987) 160–162.
- [2] N. Greiner, D. Phillips, J. Johnson, F. Volk, Diamonds in detonation soots, *Nature* 333 (1988) 440–442.

- [3] S.Jiao, A. Sumant, M. Kirk, D. Gruen, A. Krauss, O. Auciello, Microstructure of ultrananocrystalline diamond films grown by microwave ar-ch4 plasma chemical vapor deposition with or without h2, J. Applied Physics 90 (2001) 118–122.
- [4] A. Aleksenski, M. Baidakova, A. Vulš, V. Siklitskly, The structure of diamond nanoclusters, Physics of the Solid State 41 (1999) 740–743.
- [5] L. Pizzagalli, G. Galli, J. E. Klepeis, F. Gygi, Structure and stability of germanium nanoparticles, Phys. Rev. B 63 (2001) 165324.
- [6] J. Raty, G. Galli, T. V. Buuren, C. Bostedt, L. Terminello, Quantum confinement and fullerenelike surface reconstructions in nanodiamonds, Phys. Rev. Lett. 90 (2003) 037401–037404.
- [7] J. Raty, G. Galli, Ultradispersity of diamond at the nanoscale, Nature Materials 2 (2003) 792–795.
- [8] R. Car, M. Parrinello, Unified approach to molecular dynamics and density functional theory, Phys. Rev. Lett. 55 (1985) 2471–2474.
- [9] M. Casida, Recent developments and of modern density functional theory, Elsevier, Amsterdam, 1996.
- [10] X. Gonze, J. Beuken, R. Caracas, F. Detraux, M. Fuchs, G. Rignanese, L. Sindic, M. Verstraete, M. Mikamia, P. Ghosez, J. Raty, D. Allan, First principles computation of material properties : the abinit software project, Comp. Mater. Sci. 25 (2002) 478–492.
- [11] M. T. and, A microscopic model for surface induced diamond to graphite transitions, Phys. Rev. B 53 (1996) 979.
- [12] A. de Vita, G. Galli, A. Canning, R. Car, A microscopic model for surface induced diamond to graphite transitions, Nature 379 (1996) 523–526.